

## Screening of Bimetallic Heterogeneous Nanoparticle Catalysts for Arene Hydrogenation Activity under Ambient Conditions

Nicole A. Dehm, Xiaojiang Zhang, and Jillian M. Buriak\*

*Department of Chemistry, University of Alberta and the National Institute for Nanotechnology (NINT),  
Edmonton, Alberta, Canada T6G 2G2*

Received September 30, 2009

This study focuses on the application of a simple screening approach to prepare and test heterogeneous mono- and bimetallic nanoparticle (NP) catalysts for arene hydrogenation activity under ambient conditions in a quick and time efficient manner, as well as detailed testing and characterization of identified active catalysts. Over 90 mono- and bimetallic NP catalysts supported on alumina were efficiently screened for arene hydrogenation activity under ambient conditions using toluene as a model substrate. Through this approach, four catalysts were determined to be active: RhPt/Al<sub>2</sub>O<sub>3</sub>, RuPt/Al<sub>2</sub>O<sub>3</sub>, IrPt/Al<sub>2</sub>O<sub>3</sub>, and IrRh/Al<sub>2</sub>O<sub>3</sub>. These catalysts were further synthesized and tested in bulk, and RhPt/Al<sub>2</sub>O<sub>3</sub> was confirmed to be the catalyst with the highest observed rate of all the bimetallic combinations screened. Further studies were then performed, and the metal loading, temperature, pressure, and substrate to metal ratios were varied to determine the effects of these variables on the activity of the RhPt/Al<sub>2</sub>O<sub>3</sub> catalyst and a CS<sub>2</sub> poisoning study was performed on this catalyst to determine the number of active sites. From the temperature studies, the activation energy was calculated to be 30.4 kJ/mol, which is moderate when compared to other arene hydrogenation catalysts (42.0 kJ/mol for the hydrogenation of toluene with Ru NPs,<sup>1</sup> and 34.7 and 45.6 kJ/mol for benzene hydrogenation with cuboctahedral and cubic Pt NPs, respectively,<sup>2</sup> have been reported). Transmission electron microscopy (TEM), X-ray photoelectron spectroscopy (XPS), and Brunauer–Emmett–Teller (BET) surface area measurements were used to characterize the active catalysts, where it was observed that very small zero oxidation state metal NPs were well dispersed throughout the high-surface area alumina support.

### Introduction

In northern Alberta, vast areas of land contain oil sands deposits, of which bitumen is one of the main components. There are over 173 billion barrels of recoverable reserves represented by the verified deposits in Alberta, which cover approximately 140,000 km<sup>2</sup> of land.<sup>3</sup> Bitumen is composed of asphaltenes, complex arenes, cycloparaffins, and other heteroatom containing compounds of high molecular weights, all of which must be removed before most direct uses.<sup>4</sup> Specifically, hydrogenation of the large polyaromatic hydrocarbons found in bitumen is one of the steps involved in upgrading bitumen into synthetic crude oil, and thus this

challenging catalytic reaction is of great importance to the petrochemical industry.<sup>4–7</sup> This reaction is, however, difficult because of the stability of the aromatic rings, and thus harsh conditions are required in excess of 340 °C and 6.9 MPa to achieve successful hydrogenation.<sup>7</sup> Complicating matters, metal catalysts are vulnerable to poisoning because of the sulfur and nitrogen contaminants found in bitumen.<sup>8</sup> All these factors increase crude oil costs and thus it is of interest to find new families of catalysts that can function with less energy input, are sulfur and nitrogen tolerant, and are selective with respect to the desired hydrogenation products.

Nanoparticle (NP) catalysts have been used for a wide variety of reactions including both olefin<sup>9,10</sup> and arene<sup>1,2,7,8,10–62</sup>

\*To whom correspondence should be addressed. E-mail: jlburiak@ualberta.ca.

(1) Precht, M. H. G.; Scariot, M.; Scholten, J. D.; Machado, G.; Teixeira, S. R.; Dupont, J. *Inorg. Chem.* **2008**, *47*, 8995–9001.

(2) Bratlie, K. M.; Lee, H.; Komvopoulos, K.; Yang, P.; Somorjai, G. A. *Nano Lett.* **2007**, *7*, 3097–3101.

(3) Government of Alberta; <http://oilsands.alberta.ca/1.cfm>, **2009**.

(4) Song, C.; Nihonmatsu, T.; Nomura, M. *Ind. Eng. Chem. Res.* **1991**, *30*, 1726–1734.

(5) Beltramone, A. R.; Resasco, D. E.; Alvarez, W. E.; Choudhary, T. V. *Ind. Eng. Chem. Res.* **2008**, *47*, 7161–7166.

(6) Strausz, O. P.; Mojelsky, T. W.; Payzant, J. D.; Olah, G. A.; Prakash, G. K. S. *Energy Fuels* **1999**, *13*, 558–569.

(7) Owusu-Boakye, A.; Dalai, A. K.; Ferdous, D.; Adjaye, J. *Energy Fuels* **2005**, *19*, 1763–1774.

(8) Hu, L.; Xia, G.; Qu, L.; Li, M.; Li, C.; Xin, Q.; Li, D. *J. Catal.* **2001**, *202*, 220–228.

(9) Aiken, J. D.; Finke, R. G. *Chem. Mater.* **1999**, *11*, 1035–1047.

(10) Yang, X.; Yan, N.; Fei, Z.; Crespo-Quesada, R. M.; Laurenczy, G.; Kiwi-Minsker, L.; Kou, Y.; Li, Y.; Dyson, P. J. *Inorg. Chem.* **2008**, *47*, 7444–7446.

(11) Kakade, B. A.; Sahoo, S.; Halligudi, S. B.; Pillai, V. K. *J. Phys. Chem. C* **2008**, *112*, 13317–13319.

(12) Yoon, B.; Pan, H. B.; Wai, C. M. *J. Phys. Chem. C* **2009**, *113*, 1520–1525.

hydrogenations. NP catalysts are advantageous for many reasons including high surface areas and energies, unique electronic effects, and potentially lower cost: high surface to

volume ratios mean less metal is “wasted” in the particle interior, and higher selectivity produces fewer undesirable side products.<sup>63,64</sup> Both mono-<sup>1,2,11–50,65–74</sup> and bimetallic<sup>7,8,12,13,51–55,60</sup> NP catalysts have been studied for arene hydrogenation, and bimetallic catalysts are of particular interest because of the potential for enhanced activity and an increased tolerance to sulfur and nitrogen contaminants.<sup>8</sup>

While both unsupported and supported NP catalysts have demonstrated activity for arene hydrogenation, supported catalysts are more robust and also allow for easier separation of the catalyst from the reaction mixture enabling the catalyst to be easily recycled.<sup>37</sup> In addition, there are important synergistic effects between the NP catalyst and the underlying support. For example, the acidity of the support, electron transfer to and from the support, and epitaxial stress at the NP-support boundary can all have a significant influence on the activity of the catalyst.<sup>63,71,75</sup> NP catalysts have been supported on a variety of materials including carbon nanotubes<sup>11–13,55</sup> and metal oxides,<sup>7,8,14–26,51–54,60,65–71</sup> and the latter is a very common family of supports currently used for bitumen processing catalysts, among many others. Metal oxides such as Al<sub>2</sub>O<sub>3</sub>, TiO<sub>2</sub>, and SiO<sub>2</sub> are inexpensive, widely available commercially, and allow for control of parameters such as substrate acidity and porosity, among others, permitting tuning of catalyst activity.<sup>71,75</sup>

At present, a limited number of bimetallic combinations are known to be active as NP arene hydrogenation catalysts.<sup>7,8,12,13,51–55,60</sup> It would, therefore be interesting to screen a large number of bimetallic combinations, in parallel, to identify new bimetallic catalysts active for arene hydrogenation under mild conditions (1 atm H<sub>2</sub>, 22 °C). Taking into account the many possible variables, including the ratio of the two metals, metal loading, support types, substrates, and so forth, it would be incredibly time-consuming to test each individual catalyst one by one in an empirical fashion. Recently, combinatorial or high-throughput screening has

- (13) Yoon, B.; Wai, C. M. *J. Am. Chem. Soc.* **2005**, *127*, 17174–17175.
- (14) Park, I. S.; Kwon, M. S.; Kang, K. Y.; Lee, J. S.; Park, J. *Adv. Synth. Catal.* **2007**, *349*, 2039–2047.
- (15) Su, F.; Lv, L.; Lee, F. Y.; Liu, T.; Cooper, A. I.; Zhao, X. S. *J. Am. Chem. Soc.* **2007**, *129*, 14213–14223.
- (16) Lin, S. D.; Vannice, M. A. *J. Catal.* **1993**, *143*, 554–562.
- (17) Cunha, D. S.; Cruz, G. M. *Appl. Catal., A* **2002**, *236*, 55–66.
- (18) Mevellec, V.; Nowicki, A.; Roucoux, A.; Dujardin, C.; Granger, P.; Payen, E.; Philippot, K. *New J. Chem.* **2006**, *30*, 1214–1219.
- (19) Marconi, G.; Pertici, P.; Evangelisti, C.; Caporusso, A. M.; Vitulli, G.; Capannelli, G.; Hoang, M.; Turney, T. W. *J. Organomet. Chem.* **2004**, *689*, 639–646.
- (20) Spinace, E. V.; Vaz, J. M. *Catal. Commun.* **2003**, *4*, 91–96.
- (21) Yuan, T.; Fournier, A. R.; Proudlock, R.; Marshall, W. D. *Environ. Sci. Technol.* **2007**, *41*, 1983–1988.
- (22) Dominguez-Quintero, O.; Martinez, S.; Henriquez, Y.; D’Ornelas, L.; Krentzien, H.; Osuna, J. J. *Mol. Catal. A: Chem.* **2003**, *197*, 185–191.
- (23) Lang, H. F.; May, R. A.; Iversen, B. L.; Chandler, B. D. *J. Am. Chem. Soc.* **2003**, *125*, 14832–14836.
- (24) Pawelec, B.; Campos-Martin, J. M.; Cano-Serrano, E.; Navarro, R. M.; Thomas, S.; Fierro, J. L. G. *Environ. Sci. Technol.* **2005**, *39*, 3374–3381.
- (25) Marecot, P.; Mahoungou, J. R.; Barbier, J. *Appl. Catal., A* **1993**, *101*, 143–149.
- (26) Zhao, A.; Gates, B. C. *J. Catal.* **1997**, *168*, 60–69.
- (27) Schulz, J.; Roucoux, A.; Patin, H. *Chem. Commun.* **1999**, 535–536.
- (28) Schulz, J.; Roucoux, A.; Patin, H. *Chem.—Eur. J.* **2000**, *6*, 618–624.
- (29) Deshmukh, R. R.; Lee, J. W.; Shin, U. S.; Lee, J. Y.; Song, C. E. *Angew. Chem., Int. Ed.* **2008**, *47*, 8615–8617.
- (30) Mu, X. D.; Meng, J. Q.; Li, Z. C.; Kou, Y. J. *J. Am. Chem. Soc.* **2005**, *127*, 9694–9695.
- (31) Zhao, C.; Wang, H. Z.; Yan, N.; Xiao, C. X.; Mu, X. D.; Dyson, P. J.; Kou, Y. J. *J. Catal.* **2007**, *250*, 33–40.
- (32) Jacinto, M. J.; Kiyohara, P. K.; Masunaga, S. H.; Jardim, R. F.; Rossi, L. M. *Appl. Catal., A* **2008**, *338*, 52–57.
- (33) Schulz, J.; Levigne, S.; Roucoux, A.; Patin, H. *Adv. Synth. Catal.* **2002**, *344*, 266–269.
- (34) Harada, T.; Ikeda, S.; Ng, Y. H.; Sakata, T.; Mori, H.; Torimoto, T.; Matsumura, M. *Adv. Func. Mater.* **2008**, *18*, 2190–2196.
- (35) Zahmakiran, M.; Ozkar, S. *Langmuir* **2008**, *24*, 7065–7067.
- (36) Hagen, C. M.; Widegren, J. A.; Maitlis, P. M.; Finke, R. G. *J. Am. Chem. Soc.* **2005**, *127*, 4423–4432.
- (37) Widegren, J. A.; Finke, R. G. *Inorg. Chem.* **2002**, *41*, 1558–1572.
- (38) Weddle, K. S.; Aiken, J. D.; Finke, R. G. *J. Am. Chem. Soc.* **1998**, *120*, 5653–5666.
- (39) Leger, B.; Denicourt-Nowicki, A.; Roucoux, A.; Olivier-Bourbigou, H. *Adv. Synth. Catal.* **2008**, *350*, 153–159.
- (40) Pellegatta, J. L.; Blandy, C.; Colliere, V.; Choukroun, R.; Chaudret, B.; Cheng, P.; Philippot, K. *J. Mol. Catal. A: Chem.* **2002**, *178*, 55–61.
- (41) Sidhpuria, K. B.; Parikh, P. A.; Bahadur, P.; Jasra, R. V. *Ind. Eng. Chem. Res.* **2008**, *47*, 4034–4042.
- (42) Simon, L.; van Ommen, J. G.; Jentys, A.; Lercher, J. A. *J. Phys. Chem. B* **2000**, *104*, 11644–11649.
- (43) Hiyoshi, N.; Rode, C. V.; Sato, O.; Masuda, Y.; Yamaguchi, A.; Shirai, M. *Chem. Lett.* **2008**, *37*, 734–735.
- (44) Leger, B.; Denicourt-Nowicki, A.; Olivier-Bourbigou, H.; Roucoux, A. *Inorg. Chem.* **2008**, *47*, 9090–9096.
- (45) Ohde, H.; Ohde, M.; Wai, C. M. *Chem. Commun.* **2004**, 930–931.
- (46) Hiyoshi, N.; Inoue, T.; Rode, C.; Sato, O.; Shirai, M. *Catal. Lett.* **2006**, *106*, 133–138.
- (47) Graydon, W. F.; Langan, M. D. *J. Catal.* **1981**, *69*, 180–192.
- (48) Zhang, Z. G.; Okada, K.; Yamamoto, M.; Yoshida, T. *Catal. Today* **1998**, *45*, 361–366.
- (49) Lu, F.; Liu, J.; Xu, H. *Adv. Synth. Catal.* **2006**, *348*, 857–861.
- (50) Hiyoshi, N.; Osada, M.; Rode, C. V.; Sato, O.; Shirai, M. *Appl. Catal., A* **2007**, *331*, 1–7.
- (51) Venezia, A. M.; La Parola, V.; Pawelec, B.; Fierro, J. L. G. *Appl. Catal., A* **2004**, *264*, 43–51.
- (52) Wan, G.; Duan, A.; Zhao, Z.; Jiang, G.; Zhang, D.; Li, R.; Dou, T.; Chung, K. H. *Energy Fuels* **2009**, *23*, 81–85.
- (53) Thomas, J. M.; Johnson, B. F. G.; Raja, R.; Sankar, G.; Midgley, P. A. *Acc. Chem. Res.* **2003**, *36*, 20–30.
- (54) Gelman, F.; Avnir, D.; Schumann, H.; Blum, J. J. *Mol. Catal. A: Chem.* **2001**, *171*, 191–194.
- (55) Pawelec, B.; La Parola, V.; Navarro, R. M.; Murcia-Mascaros, S.; Fierro, J. L. G. *Carbon* **2006**, *44*, 84–98.
- (56) Roucoux, A.; Schulz, J.; Patin, H. *Chem. Rev.* **2002**, *102*, 3757–3778.
- (57) Barbaro, P.; Bianchini, C.; Dal Santo, V.; Meli, A.; Moneti, S.; Psaro, R.; Scaffidi, A.; Sordelli, L.; Vizza, F. *J. Am. Chem. Soc.* **2006**, *128*, 7065–7076.
- (58) Hiyoshi, N.; Miura, R.; Rode, C. V.; Sato, O.; Shirai, M. *Chem. Lett.* **2005**, *34*, 424–425.
- (59) Barbaro, P.; Bianchini, C.; Dal Santo, V.; Meli, A.; Moneti, S.; Pirovano, C.; Psaro, R.; Sordelli, L.; Vizza, F. *Organometallics* **2008**, *27*, 2809–2824.
- (60) Fujikawa, T.; Idei, K.; Ebihara, T.; Mizuguchi, H.; Usui, K. *Appl. Catal., A* **2000**, *192*, 253–261.
- (61) Roucoux, A. *Top. Organomet. Chem.* **2005**, *16*, 261–279.
- (62) Liang, C.; Zhao, A.; Zhang, X.; Ma, Z.; Prins, R. *Chem. Commun.* **2009**, 2047–2049.
- (63) Narayanan, R.; El-Sayed, M. A. *J. Phys. Chem. B* **2005**, *109*, 12663–12676.
- (64) Yoo, J. W.; Hathcock, D. J.; El-Sayed, M. A. *J. Catal.* **2003**, *214*, 1–7.
- (65) Gao, H.; Angelici, R. J. *J. Am. Chem. Soc.* **1997**, *119*, 6937–6938.
- (66) Ioannides, T.; Verykios, X. E. *J. Catal.* **1993**, *143*, 175–186.
- (67) Crump, C. J.; Gilbertson, J. D.; Chandler, B. D. *Top. Catal.* **2008**, *49*, 233–240.
- (68) Lin, S. D.; Vannice, M. A. *J. Catal.* **1993**, *143*, 539–553.
- (69) Takagi, H.; Isoda, T.; Kusakabe, K.; Morooka, S. *Energy Fuels* **1999**, *13*, 1191–1196.
- (70) Santana, R. C.; Jongpatiwut, S.; Alvarez, W. E.; Resasco, D. E. *Ind. Eng. Chem. Res.* **2005**, *44*, 7928–7934.
- (71) Pawelec, B.; Castano, P.; Arandes, J. M.; Bilbao, J.; Thomas, S.; Pena, M. A.; Fierro, J. L. G. *Appl. Catal., A* **2007**, *317*, 20–33.
- (72) Park, K. H.; Jang, K.; Kim, H. J.; Son, S. U. *Angew. Chem., Int. Ed.* **2007**, *46*, 1152–1155.
- (73) Yang, S. Y.; Stock, L. M. *Energy Fuels* **1998**, *12*, 644–648.
- (74) Widegren, J. A.; Finke, R. G. *J. Mol. Catal. A: Chem.* **2003**, *198*, 317–341.
- (75) Bertolini, J.-C.; Rousset, J.-L. *Nanomaterials and Nanochemistry*; Springer: New York, 2008.

proven to be an efficient means of synthesizing and screening large numbers of potential materials for a desired property, leading to much shorter discovery times.<sup>76–89</sup> For example, Maier used IR thermography to simultaneously screen 37 potential catalysts for 1-hexyne hydrogenation and isooctane oxidation activity in the gas phase.<sup>81</sup> More recently Parkinson used an ink jet printer to print overlapping oxide precursors onto conductive glass substrates. These materials were then screened for photoelectrolysis activity, and a potential catalyst was identified.<sup>78</sup> On the basis of the prior success and potential of the combinatorial approach for catalyst synthesis and testing, a library of potential catalysts could be prepared and tested for arene hydrogenation activity under ambient conditions, allowing for efficient identification of active catalysts.

In the present study, a variety of mono- and bimetallic NP catalysts supported on alumina were synthesized and assessed using a simple parallel screening approach, under ambient conditions, for toluene hydrogenation activity. In total, 91 catalysts were screened using 13 representative transition metals from the first, second, and third rows of the periodic table. One particularly active catalyst was identified and further characterized in bulk and studied (kinetics and materials characterizations) and is described here.

## Experimental and Methods

**Materials.**  $\text{CuCl}_2 \cdot 2\text{H}_2\text{O}$  (99.999%-Cu),  $\text{CrCl}_3 \cdot 6\text{H}_2\text{O}$ ,  $\text{HAuCl}_4 \cdot x\text{H}_2\text{O}$  (99.9985%-Au),  $\text{RuCl}_3 \cdot x\text{H}_2\text{O}$  (99.9%-Ru),  $\text{IrCl}_3 \cdot x\text{H}_2\text{O}$  (99.9%-Ir),  $\text{MnCl}_2 \cdot 4\text{H}_2\text{O}$  (99.999%-Mn),  $\text{PdCl}_2$  (99.9%-Pd),  $\text{CoCl}_2 \cdot 6\text{H}_2\text{O}$  (99.999%-Co),  $\text{Na}_2\text{PtCl}_4 \cdot x\text{H}_2\text{O}$ ,  $\text{NiCl}_2 \cdot 6\text{H}_2\text{O}$  (99.999+%-Ni),  $\text{FeCl}_2 \cdot 4\text{H}_2\text{O}$  (99%),  $\text{MoCl}_5$  (anhydrous, 99.6%),  $\text{RhCl}_3 \cdot x\text{H}_2\text{O}$  (38–41% Rh), and 0.5% Rh/ $\text{Al}_2\text{O}_3$  (pellets) were purchased from Strem Chemicals and were used without further purification. Aluminum-*sec*-butoxide (95%), decahydronaphthalene, *cis* + *trans* (97%), and methylcyclohexane (99+%) were purchased from Alfa Aesar. Ethanol (100%, anhydrous) was purchased from Commercial Alcohol. Millipore water was used throughout. Hydrochloric acid (concentrated), and silica gel were purchased from EMD. Dichloromethane (ACS), isopropanol, toluene were purchased from

Fischer Scientific. Carbon disulfide was purchased from Sigma-Aldrich and was used without further purification. Isopropanol was dried over molecular sieves and stored under argon before use. Toluene was purified through a solvent purification system and was stored under argon until used. Hydrogen, argon, and 5% hydrogen/95% argon were supplied by Praxair.

**Instrumentation.** A Varian CP-3800 Gas Chromatograph with a CP-4800 autosampler with a fused silica capillary column and a FID detector was used to analyze the samples of the reaction mixture. A Corning Model PC-420 Laboratory stirrer/hot plate was used throughout, except for the temperature studies, in which an IKA Works Ceramag Midi stirrer/hot plate with an IKA ETS-D4 temperature sensor was used for temperatures above ambient. An Agilent 6890 gas chromatography with a 5973 mass detector was used for the GC-MS experiments. A Parr pressure vessel, model 4774-T-SS-3000 and a model 4838 controller with a pressure display module were used for the pressure and  $\text{CS}_2$  poisoning studies. For the transmission electron microscopy (TEM) analysis, a JEOL JEM-2200FS was used in STEM mode. For X-ray photoelectron spectroscopy (XPS) a Kratos Analytical, Axis-Ultra instrument was used for the sample analysis. XPS were performed under UHV conditions ( $< 10^{-8}$  Torr). Surface areas were measured by nitrogen adsorption at 77.3 K using an Autosorb-1 high performance surface area and pore size analyzer (Quantachrome Instruments).

**Catalyst Screening Synthesis of 1 mol % Metal Loading.** The procedure for the catalyst synthesis was based on modified procedures established by Maier.<sup>81,90</sup> 0.133 M solutions of the required metal salts in ethanol were prepared, as was a 1.788 M solution of aluminum-*sec*-butoxide in dichloromethane and a solution consisting of 1.0 mL of ethanol, 13  $\mu\text{L}$  of concentrated hydrochloric acid, and 71  $\mu\text{L}$  of water. The sample holders (Supporting Information, Figure S2) were centered on the stir plate, and glass coated stir bars (5 mm  $\times$  6 mm) were added to each well. The desired amount of each metal salt solution was added quickly (in under one second) to each well to give the desired metal loading and ratio of the two metals (e.g., 10  $\mu\text{L}$  of each metal salt solution would give a 50:50 ratio of the two metals with a total metal loading of 1 mol %). Then 300  $\mu\text{L}$  of ethanol followed by 298  $\mu\text{L}$  of 1.788 M aluminum-*sec*-butoxide were quickly (under 1 s) added to each well via pipet. After stirring for approximately 5 min, 218  $\mu\text{L}$  of the ethanol/hydrochloric acid/water solution was quickly (under one second) added. Each sample holder was covered with parafilm; the parafilm was punctured several times above each well, and the solution was allowed to age and dry overnight in laboratory ambient conditions. After processing, each sample holder was placed in a vial, which was capped with a septum (Supporting Information, Figure S2).

**Batch Catalyst Synthesis of 1 mol % Metal Loading.** The catalyst screening synthesis was scaled up, and the catalyst was prepared in a 100 mL polypropylene beaker with a Teflon coated stir bar. After processing, the powder was transferred to a vial for immediate use or stored under argon.

**Processing.** All catalysts were calcined in air in a tube furnace using the following program: heat to 65  $^\circ\text{C}$  (rate 1  $^\circ\text{C}/\text{min}$ ), hold at 65  $^\circ\text{C}$  for 30 min, heat to 250  $^\circ\text{C}$  (rate 1  $^\circ\text{C}/\text{min}$ ), hold at 250  $^\circ\text{C}$  for 3 h, cool to 25  $^\circ\text{C}$  (rate 1  $^\circ\text{C}/\text{min}$ ). Then the catalyst was hydrogen annealed under a 5%  $\text{H}_2/95\%$  Ar atmosphere as follows: heat to 300  $^\circ\text{C}$  (rate 5  $^\circ\text{C}/\text{min}$ ), hold at 300  $^\circ\text{C}$  for 3 h, cool down to 25  $^\circ\text{C}$  rapidly by opening the furnace.

**Screening.** A solution of 7.7 mL of isopropanol, 0.456 mL of decahydronaphthalene (internal standard), and 0.308 mL of toluene was prepared. A necessary number of lines on the

(76) Wang, J.; Yoo, Y.; Gao, C.; Takeuchi, I.; Sun, X.; Chang, H.; Xiang, X.-D.; Schultz, P. G. *Science* **1998**, 279, 1712–1715.

(77) Danielson, E.; Devenney, M.; Giaquinta, D. M.; Golden, J. H.; Haushalter, R. C.; McFarland, E. W.; Poojary, D. M.; Reaves, C. M.; Weinberg, W. H.; Wu, X. D. *Science* **1998**, 279, 837–840.

(78) Woodhouse, M.; Parkinson, B. A. *Chem. Mater.* **2008**, 20, 2495–2502.

(79) Tai, C. C.; Chang, T.; Roller, B.; Jessop, P. G. *Inorg. Chem.* **2003**, 42, 7340–7341.

(80) Xiang, X. D.; Sun, X.; Briceno, G.; Lou, Y.; Wang, K. A.; Chang, H.; Wallace-Freedman, W. G.; Chen, S. W.; Schultz, P. G. *Science* **1995**, 268, 1738–1740.

(81) Holzwarth, A.; Schmidt, H. W.; Maier, W. F. *Angew. Chem., Int. Ed.* **1998**, 37, 2644–2647.

(82) Orschel, M.; Klein, J.; Schmidt, H. W.; Maier, W. F. *Angew. Chem., Int. Ed.* **1999**, 38, 2791–2794.

(83) Klein, J.; Lehmann, C. W.; Schmidt, H. W.; Maier, W. F. *Angew. Chem., Int. Ed.* **1998**, 37, 3369–3373.

(84) Kirsten, G.; Maier, W. F. *Appl. Surf. Sci.* **2004**, 223, 87–101.

(85) Scheidtmann, J.; Weib, P. A.; Maier, W. F. *Appl. Catal., A* **2001**, 222, 79–89.

(86) Maier, W. F. *Angew. Chem., Int. Ed.* **1999**, 38, 1216–1218.

(87) Maier, W. F.; Stowe, K.; Sieg, S. *Angew. Chem., Int. Ed.* **2007**, 46, 6016–6067.

(88) Danielson, E.; Golden, J. H.; McFarland, E. W.; Reaves, C. M.; Weinberg, W. H.; Wu, X. D. *Nature* **1997**, 389, 944–948.

(89) Briceno, G.; Chang, H.; Sun, X.; Schultz, P. G.; Xiang, X. D. *Science* **1995**, 270, 273–275.

(90) Klein, J.; Lettmann, C.; Maier, W. F. *J. Non-Cryst. Solids* **2001**, 282, 203–220.



Schlenk line were split with Y joints, and additional tubes were attached. A syringe barrel was inserted into the end of each tube, and a needle was attached to each syringe. As described earlier (Catalyst screening synthesis of 1 mol % metal loading) each sample holder containing the prepared catalyst is located in an individual vial. The septum on each vial was pierced with a needle that was attached to the Schlenk line (Supporting Information, Figure S3). The vials underwent three of the following cycles: the vials were placed under vacuum and then backfilled with Ar. This was repeated with Ar and then with H<sub>2</sub>. One milliliter of isopropanol was added to the bottom of each vial (but not to the sample holder), to minimize evaporation losses from the sample holder. Next, 0.77 mL of the previously prepared solution was added to each sample holder. The vials were stirred for 4 h under 1 atm H<sub>2</sub> pressure and at 22 °C. After 4 h, each sample holder was removed from the vial. As much of the reaction mixture as possible was removed from the sample holder with a Pasteur pipet. The reaction mixture was filtered through a different Pasteur pipet packed with a small amount silica gel directly into a GC vial. The substrate and products were diluted with 1.0 mL of dichloromethane. The screening hydrogenation results obtained for Rh<sub>0.5</sub>Pt<sub>0.5</sub>/Al<sub>2</sub>O<sub>3</sub> were performed in triplicate.

**General Batch Hydrogenation.** The appropriate amount of catalyst to give  $3.8 \times 10^{-5}$  mol of metal was added to a 25 mL 3 neck round-bottomed flask. A glass coated stir bar was added, and the flask was capped with two septa and a gas adapter. The flask was placed under vacuum and then backfilled with Ar; this was repeated two more times with Ar. Next, 10.0 mL of isopropanol was added. The flask was placed under vacuum and then backfilled with H<sub>2</sub> for a total of three times. A 0.59 mL portion ( $3.8 \times 10^{-3}$  mol) of decahydronaphthalene and 0.40 mL ( $3.8 \times 10^{-3}$  mol) of toluene were added by syringe, and the reaction was stirred under ambient conditions (1 atm H<sub>2</sub>, 22 °C). The reaction was monitored every 15 min for the first 2 h, and then every hour for an additional 5 h via gas chromatography (GC). To prepare samples for GC analysis, 0.4 mL samples of the reaction mixture were removed from the flask with a syringe. The contents of the syringe were filtered through a silica gel filter as previously described. The bulk hydrogenation results obtained for Rh<sub>0.5</sub>Pt<sub>0.5</sub>/Al<sub>2</sub>O<sub>3</sub> were performed in triplicate.

**Batch Toluene Studies.** The hydrogenation was performed as specified in the procedure for general batch hydrogenation, with varying amounts of toluene depending on the desired ratio of catalyst to substrate.

**Batch Temperature Studies.** The hydrogenation was performed as specified in the procedure for general batch hydrogenation, except that if heating the reaction mixture above room temperature, a reflux condenser was attached to the middle neck of the round-bottom flask and a gas adapter was connected to the top of the reflux condenser. The other two necks on the round-bottom flask were sealed with septa. For cooling below room temperature, an ice bath was used to achieve a temperature of 0 °C, and a bath consisting of dioxane and CO<sub>2</sub> (s) was used for a 10 °C bath.

**Batch Pressure Studies.** The quantities of catalyst, solvent, and substrate were scaled up by a factor of 2 for the batch pressure studies, and decahydronaphthalene was not added. The catalyst was added to the stainless steel bottom of the pressure reactor, and then isopropanol and toluene were sequentially added. The pressure reactor was assembled, and hydrogen was gently flowed through the reactor for 30 s. Then the reactor was sealed, pressurized to the desired pressure, and the course of the reaction was monitored via a Parr pressure controller interfaced with a computer. After the reaction was complete, the reactor was disassembled, and a sample of the reaction mixture was analyzed by gas chromatography as previously described.

**CS<sub>2</sub> Poisoning Studies.** The following CS<sub>2</sub> poisoning studies were done based on a modified procedure by Hornstein et al. and were performed in triplicate.<sup>91</sup> A 0.3893 g portion of the Rh<sub>0.5</sub>Pt<sub>0.5</sub>/Al<sub>2</sub>O<sub>3</sub> catalyst or 0.782 g of the 0.5% Rh/Al<sub>2</sub>O<sub>3</sub> catalyst was weighed into a clean 20 mL beaker. A glass coated stir bar was added to the beaker followed by 5.0 mL of isopropanol. A 0.038 M solution of CS<sub>2</sub> in isopropanol was prepared fresh each day, and the required amount of the solution was added to the beaker. Ratios of 0, 0.02, 0.04, 0.06, and 0.08 mol CS<sub>2</sub>/mol total metal were used for the Rh<sub>0.5</sub>Pt<sub>0.5</sub>/Al<sub>2</sub>O<sub>3</sub> catalyst, and ratios of 0, 0.01, 0.02, 0.03, and 0.04 mol CS<sub>2</sub>/mol total metal were used for the commercial catalyst 0.5% Rh/Al<sub>2</sub>O<sub>3</sub>. Then an additional 5.0 mL of isopropanol was added to the beaker followed by 0.40 mL of toluene. Decahydronaphthalene was not added. The beaker was placed into the bottom of the Parr reactor with the hydrogen inlet placed directly in the reaction solution, and then the reactor was assembled. The Parr reactor was sealed, and the solution was stirred for 30 s at a stir speed of 7. Then the stirrer was turned off, and hydrogen gas was gently flowed through the reactor for 30 s. The reactor was then sealed and pressurized to 5 atm. The course of the reaction was monitored via a Parr pressure controller interfaced with a computer for 1 h. After 1 h, the reactor was depressurized and disassembled.

**Sample Preparation for XPS, TEM, and BET.** XPS: The dried sample was first finely grounded to reduce the particle size. The ground powders were then placed into a die and pressed into a pellet under high pressure. The pellet was then used for XPS analysis. TEM (before hydrogenation): Raw samples were carefully ground with a mortar and pestle for 20 min. The average particle size is less than 100 nm after ground. A small amount of the ground powder was then mounted on a carbon-coated grid for TEM analysis. TEM (after hydrogenation): After reaction, the solvent was removed/vaporized under vacuum overnight. The raw sample was then ground and sprayed on a carbon coated TEM grid. Brunauer–Emmett–Teller (BET): Before analysis, samples were degassed at 250 °C for 23 h under vacuum.

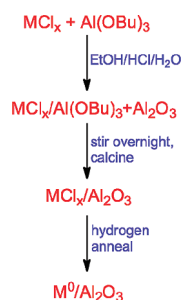
## Results and Discussion

The field of arene hydrogenation is well established industrially with a variety of heterogeneous catalysts being used (e.g., CoMo, MoW, and NiMo supported on alumina),<sup>4,7,92</sup> but relatively harsh conditions are required to achieve required catalyst activities. As a result, there has been interest in developing catalysts that are active under milder conditions. For example, Rh NPs stabilized by copolymers demonstrated a TOF (turnover frequency) of 250 h<sup>-1</sup> and a TTO (total turnover) of 20 000 mol/mol Rh for benzene hydrogenation at 40 bar H<sub>2</sub> and 75 °C.<sup>30,31</sup> Magnetically recoverable Rh NPs were very active for benzene hydrogenation with a TOF of 825 h<sup>-1</sup> at 6 atm H<sub>2</sub> and 75 °C.<sup>32</sup> Pillai reported a TOF of 6600 h<sup>-1</sup> for benzene hydrogenation and 4950 h<sup>-1</sup> for toluene hydrogenation at 20 bar H<sub>2</sub> and 40 °C using Rh NPs on multiwalled carbon nanotubes.<sup>11</sup> Ambient conditions (1 atm H<sub>2</sub>, 22 °C), however, are obviously the most challenging for arene hydrogenation, and there are very few examples in the literature.<sup>18,19,27–29,72</sup> For example, Roucoux showed that unsupported Rh NPs were active for benzene and toluene hydrogenation under ambient conditions (1 atm H<sub>2</sub>, 20 °C) with TOFs of 57 h<sup>-1</sup> and 53 h<sup>-1</sup>, respectively (TOF reported as mol H<sub>2</sub> per mol of Rh).<sup>27</sup> To discover new leads toward

(91) Hornstein, B. J.; Aiken, J. D.; Finke, R. G. *Inorg. Chem.* **2002**, *41*, 1625–1638.

(92) Cooper, B. H.; Donnis, B. B. L. *Appl. Catal., A* **1996**, *137*, 203–223.

Scheme 1. Scheme Depicting the Steps for Catalyst Synthesis



discovery of supported heterogeneous arene hydrogenation catalysts that are active under ambient conditions, we applied a parallel synthesis and screening approach.

Supported NP catalysts have been made by a variety of methods, with one of the more common based upon impregnation of an existing oxide supports.<sup>18,20,64</sup> Another approach involves a multistep synthesis utilizing preformed stabilized NPs that are then absorbed to the support.<sup>64</sup> In contrast, the in situ one pot method used by Maier involves synthesizing the NPs and the support simultaneously; the metal precursors and the water-sensitive metal alkoxide are mixed together and processed in one batch (Scheme 1).<sup>81</sup> These steps were followed by hydrolysis and condensation of the metal alkoxide to give the metal oxide in which the metal precursor is encapsulated. The metal precursor is not reduced to NPs until the hydrogen anneal step is performed, leading to reduced metal NPs on a metal oxide support. The advantage of this approach is that it is a one-pot method, no stabilizer is required for the NPs to form, and it can be performed in laboratory ambient conditions, further simplifying the procedure.

**Catalyst Synthesis and Screening.** Metal chloride salts were used as the NP precursors, and over 90 mono- and bimetallic NP catalysts were synthesized and tested for arene hydrogenation activity based on the reaction shown at the top of Figure 1. Since the goal of this work was the development of air stable, easily handled and synthesized catalysts, all steps involved exposure to an open atmosphere. Our initial screening apparatus utilized a multi-well glass plate, as shown in Figure S1 in the Supporting Information, but cross-contamination by the volatile toluene precursor and methylcyclohexane product led to spurious results; a system that isolates each vessel was required in which each vessel has its own separate gas supply (Figures S2 and S3, Supporting Information). To allow for easy identification of the active catalysts and simple interpretation of the results, a visualization approach of the data was used, with the results shown in Figure 1. The reactions were commenced and arrested after 4 h to identify active catalyst combinations.

As can be seen from the side view of the bar graphs shown in Figure 1b, there are several catalysts that are active, and a large number of inactive combinations under the screening conditions. From the top down view of the 3D bar graph (Figure 1a), it can be easily identified that bimetallic catalysts containing Rh were the most consistent for activity, with the exception of the RhCu combination. The deactivation of a catalytically active metal upon alloying with Cu has been observed before with a PtCu bimetallic catalyst, and was attributed to an

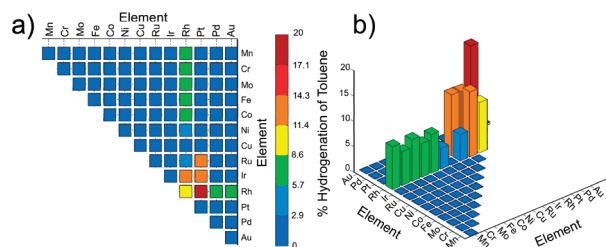
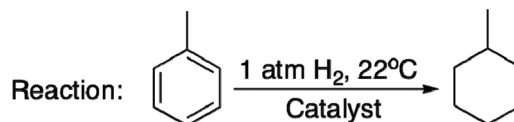


**Figure 1.** 3D bar graphs (a, top down view) and (b, side view) of screening results. The *x*- and *y*-axes represent the different transition metals used, with the *z*-axis showing the percent hydrogenation after 4 h.

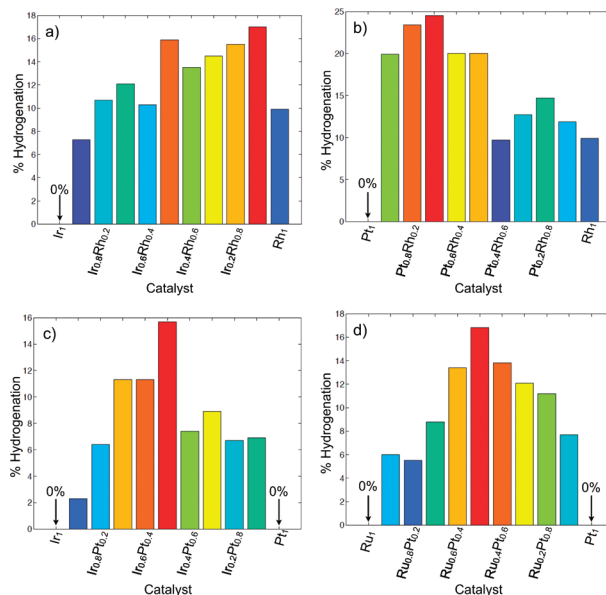


**Figure 2.** Bar graphs with varying ratios of metals, metal loading held constant at 1 mol %. (a) IrRh/Al<sub>2</sub>O<sub>3</sub>, (b) RhPt/Al<sub>2</sub>O<sub>3</sub>, (c) IrPt/Al<sub>2</sub>O<sub>3</sub>, (d) RuPt/Al<sub>2</sub>O<sub>3</sub>. The percent hydrogenation was measured after 4 h.

enrichment of catalytically inactive copper on the surface of the NPs.<sup>93</sup> From the screening results, the most active catalysts were identified to be Rh<sub>0.5</sub>Pt<sub>0.5</sub>/Al<sub>2</sub>O<sub>3</sub>, Ir<sub>0.5</sub>Pt<sub>0.5</sub>/Al<sub>2</sub>O<sub>3</sub>, Ru<sub>0.5</sub>Pt<sub>0.5</sub>/Al<sub>2</sub>O<sub>3</sub>, Ir<sub>0.5</sub>Rh<sub>0.5</sub>/Al<sub>2</sub>O<sub>3</sub>, and Rh<sub>1</sub>/Al<sub>2</sub>O<sub>3</sub> in order of highest activity to lowest activity, and the results obtained for Rh<sub>0.5</sub>Pt<sub>0.5</sub>/Al<sub>2</sub>O<sub>3</sub> were performed in triplicate. It is of note that the monometallic Ru<sub>1</sub>/Al<sub>2</sub>O<sub>3</sub>, Pt<sub>1</sub>/Al<sub>2</sub>O<sub>3</sub> and Ir<sub>1</sub>/Al<sub>2</sub>O<sub>3</sub> catalysts were inactive for the hydrogenation of toluene under these conditions, but upon alloying with Rh or Pt, the bimetallic catalysts exhibited a higher activity than either of their parent metals.

From the screening results, the four most active bimetallic catalysts (Rh<sub>0.5</sub>Pt<sub>0.5</sub>/Al<sub>2</sub>O<sub>3</sub>, Ir<sub>0.5</sub>Pt<sub>0.5</sub>/Al<sub>2</sub>O<sub>3</sub>, Ru<sub>0.5</sub>Pt<sub>0.5</sub>/Al<sub>2</sub>O<sub>3</sub>, and Ir<sub>0.5</sub>Rh<sub>0.5</sub>/Al<sub>2</sub>O<sub>3</sub>) were then screened again using varying ratios of the two metals in 10% increments while holding the metal loading constant at 1 mol %. These results are shown in Figure 2. In the case of IrRh

(93) Hoover, N. N.; Auten, B. J.; Chandler, B. D. *J. Phys. Chem. B* **2006**, *110*, 8606–8612.

**Table 1.** Batch Toluene Hydrogenation Results from First Generation Screening.<sup>a</sup>

entry	catalyst <sup>b</sup>	obs. rate [h <sup>-1</sup> ]	% conv. (2 h)	% conv. (7 h)
1	Rh <sub>1</sub>	7.7	17.8	58
2	Ir <sub>0.5</sub> Rh <sub>0.5</sub>	11.1	22.8	36
3	Ir <sub>0.5</sub> Pt <sub>0.5</sub>	12.8	27.2	47
4	Ru <sub>0.5</sub> Pt <sub>0.5</sub>	12.4	23.1	52
5	Rh <sub>0.5</sub> Pt <sub>0.5</sub> <sup>c</sup>	24.9	51.3	90
6	Rh <sub>0.5</sub> Pt <sub>0.5</sub> <sup>d</sup>	14.6	26.2	54
7	Rh <sub>0.25</sub> Pt <sub>0.25</sub>	27.1	45.4	85.3
8	Rh <sub>1</sub> Pt <sub>1</sub>	6.2	14.4	46.0
9	Rh <sub>2.5</sub> Pt <sub>2.5</sub>	5.0	12.2	42.9

<sup>a</sup> Reaction conditions:  $3.8 \times 10^{-5}$  mol metal, 10.0 mL of isopropanol substrate/cat. = 100:1 =  $3.8 \times 10^{-3}$  mol toluene, 22 °C, 1 atm H<sub>2</sub>. <sup>b</sup> All catalysts were supported on Al<sub>2</sub>O<sub>3</sub>, with the subscripts indicating the mol % of the metals. <sup>c</sup> Observed rate based on results obtained in triplicate. <sup>d</sup> Ethanol used as the solvent instead of isopropanol.

(Figure 2a), the more active catalysts were those that are richer in Rh, whereas with RhPt (Figure 2b) the more active catalysts were those that were richer in Pt. In contrast to these trends, with IrPt and RuPt (Figure 2c and 2d), the most active catalysts were those that have approximately equal amounts of the two metals.

The five most active catalysts (Rh<sub>0.5</sub>Pt<sub>0.5</sub>/Al<sub>2</sub>O<sub>3</sub>, Ir<sub>0.5</sub>Pt<sub>0.5</sub>/Al<sub>2</sub>O<sub>3</sub>, Ru<sub>0.5</sub>Pt<sub>0.5</sub>/Al<sub>2</sub>O<sub>3</sub>, Ir<sub>0.5</sub>Rh<sub>0.5</sub>/Al<sub>2</sub>O<sub>3</sub>, and Rh<sub>1</sub>/Al<sub>2</sub>O<sub>3</sub>) were synthesized and tested in bulk to confirm their activity with the results shown in Table 1. Toluene hydrogenation reactions were performed at atmospheric pressure and temperature in laboratory batch reactors. The progress of the reactions was monitored through gas chromatography in which no partially hydrogenated intermediates were detected, only the fully hydrogenated product of methylcyclohexane, which was also confirmed for a representative reaction by GC-MS. The observed rate (obs. rate) relative to the methylcyclohexane hydrogenation product was calculated during the first 2 h of hydrogenation results, where

$$\text{obs. rate} = \frac{\text{mol methylcyclohexane/mol metal in catalyst}}{\text{time(h)}}$$

As can be seen from Table 1, entries 1–5, Rh<sub>0.5</sub>Pt<sub>0.5</sub>/Al<sub>2</sub>O<sub>3</sub> was confirmed to be the most active catalyst with an observed rate of  $24.9 \pm 2.8 \text{ h}^{-1}$  based on experiments performed in triplicate. The next most active catalysts were determined to be Ir<sub>0.5</sub>Pt<sub>0.5</sub>/Al<sub>2</sub>O<sub>3</sub> and Ru<sub>0.5</sub>Pt<sub>0.5</sub>/Al<sub>2</sub>O<sub>3</sub> followed by Ir<sub>0.5</sub>Rh<sub>0.5</sub>/Al<sub>2</sub>O<sub>3</sub>. The trends in bulk activity correspond well with the trends observed for the screening results (Supporting Information, Figure S4), validating the screening results. While none of these bimetallic catalysts have been previously reported as arene hydrogenation catalysts with the exception of RuPt (Midgley reported Ru<sub>5</sub>Pt<sub>1</sub> and Ru<sub>10</sub>Pt<sub>2</sub> to be successful benzene hydrogenation catalysts at 80 °C and 20 bar H<sub>2</sub> pressure<sup>53</sup>), it is of note that RuPt NPs have been previously used as a catalyst for preferential CO oxidation in the presence of hydrogen feeds,<sup>94,95</sup> RhPt NPs

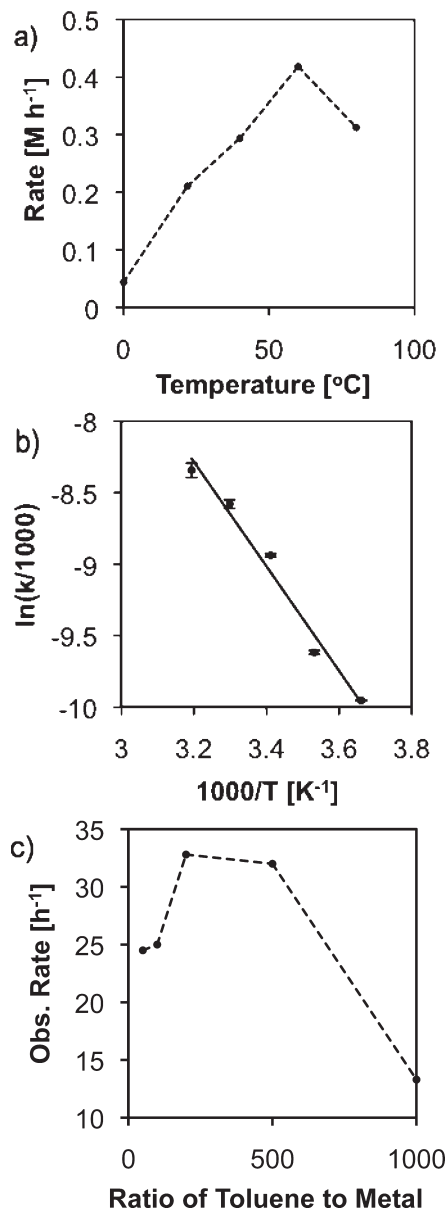


**Figure 3.** (a) Rate as a function of temperature for the hydrogenation of toluene. (b) Arrhenius plot, with the slope of the trend line equaling  $-3.65$ . (c) Observed rate as a function of the ratio of toluene to metal. Lines within the plots are drawn merely as a visual aid.

have been used as CO oxidation catalysts,<sup>96,97</sup> and the RhPt combination has been used as an electrocatalyst for the dehydrogenative oxidation of cyclohexane to benzene.<sup>98</sup>

**Discussion of Catalytic Activity.** Since the RhPt bimetallic combination led to the highest observed rate, this catalyst system was studied in further detail. Toluene hydrogenation reactions were performed on the alumina supported RhPt bimetallic catalyst in bulk in a laboratory batch reactor. Observed rates were measured during the first 2 h of the hydrogenation reaction and normalized against the number of moles of metal in the catalyst. A number of parameters were varied, including metal loading,

(94) Alayoglu, S.; Nilekar, A. U.; Mavrikakis, M.; Eichhorn, B. *Nat. Mater.* **2008**, *7*, 333–338.

(95) Alayoglu, S.; Eichhorn, B. *J. Am. Chem. Soc.* **2008**, *130*, 17479–17486.

(96) Abdelsayed, V.; Aljarash, A.; El-Shall, M. S.; Al Othman, Z. A.; Alghamdi, A. H. *Chem. Mater.* **2009**, *21*, 2825–2834.

(97) Park, J. Y.; Zhang, Y.; Grass, M.; Zhang, T.; Somorjai, G. A. *Nano Lett.* **2008**, *8*, 673–677.

(98) Kim, H. J.; Choi, S. M.; Nam, S. H.; Seo, M. H.; Kim, W. B. *Appl. Catal., A* **2009**, *352*, 145–151.



**Table 2.** Summary of the CS<sub>2</sub> Poisoning Results and Catalytic Activities of the Prepared Rh<sub>0.5</sub>Pt<sub>0.5</sub>/Al<sub>2</sub>O<sub>3</sub> and Commercial 0.5% Rh/Al<sub>2</sub>O<sub>3</sub> Catalysts<sup>a</sup>

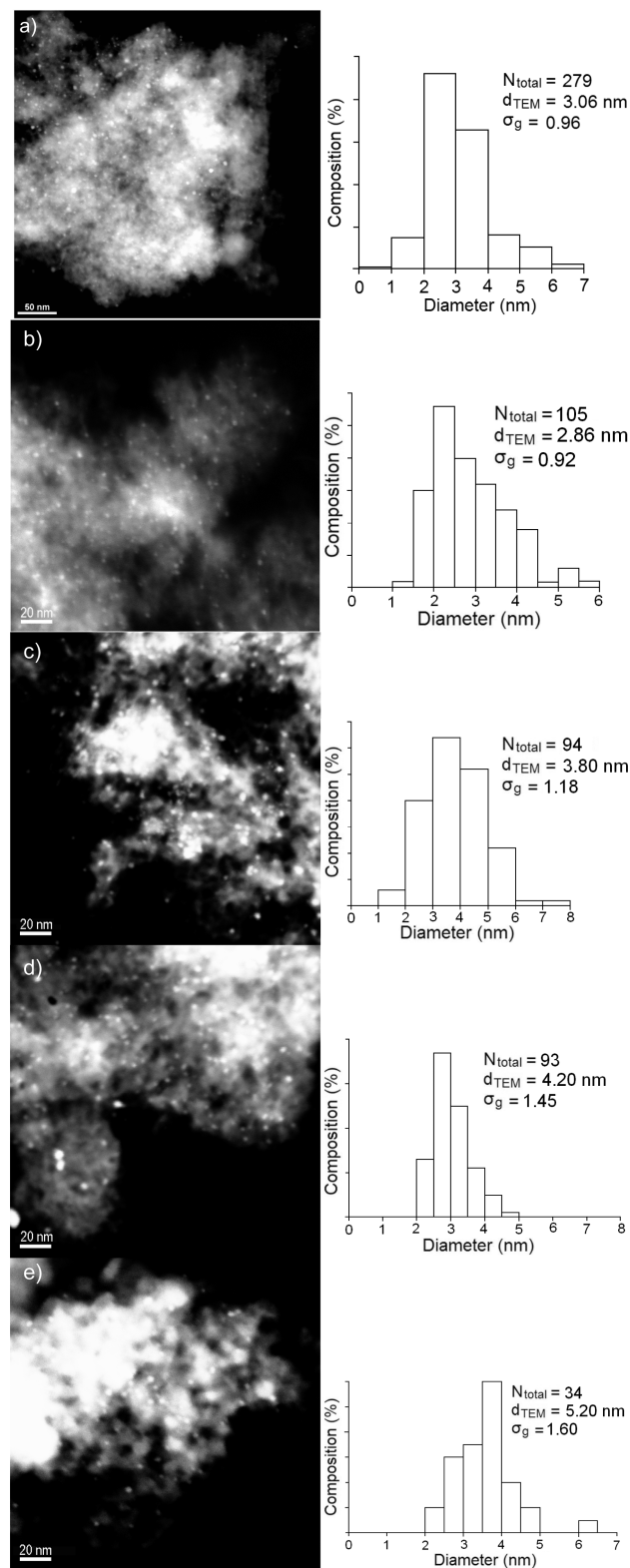
	Rh <sub>0.5</sub> Pt <sub>0.5</sub> /Al <sub>2</sub> O <sub>3</sub>	0.5% Rh/Al <sub>2</sub> O <sub>3</sub>
rate <sup>b</sup>	0.76 ± 0.16 psi/h	0.47 ± 0.13 psi/h
TOF	43.8 h <sup>-1</sup>	27.2 h <sup>-1</sup>
mol CS <sub>2</sub> /mol total metal <sup>c</sup>	0.081	0.046
TOF (corrected) <sup>d</sup>	108 h <sup>-1</sup>	118 h <sup>-1</sup>
rel. TOF	1	1.09

<sup>a</sup> Catalytic activities measured at 5 atm H<sub>2</sub> pressure, 295 K. <sup>b</sup> Values based on  $3.8 \times 10^{-5}$  mol of total metal. <sup>c</sup> Ratio of mol CS<sub>2</sub>/mol total metal required to deactivate catalyst. Determined from results shown in Supporting Information, Figure S6. <sup>d</sup> TOF is corrected for active Rh and Pt atoms determined by CS<sub>2</sub> poisoning and using a 1/5 position/metal stoichiometry ratio, as previously described by Hornstein et al.<sup>91</sup>

temperature, amount of substrate, and hydrogen pressure, to determine the effect these variables would have on the observed rates of the RhPt catalyst. A CS<sub>2</sub> poisoning study was also performed on the RhPt catalyst to determine the number of catalytically active sites in the catalyst.<sup>91</sup> The hydrogenation of toluene was performed using ethanol as solvent (Table 1, entry 6), and a decrease in the observed rate of the catalyst was observed; therefore isopropanol was used as the solvent for the remainder of this study. The metal loading of the RhPt catalyst was varied between 0.5% and 5% while holding the ratios of Rh and Pt constant (Table 1, entries 7–9). It was found that the observed rate increased slightly as the loading was decreased to 0.5% but with metal loadings of 2% and 5%, the observed rate greatly decreased.

The temperature of the hydrogenation reaction was increased to determine the range of temperatures in which the catalyst was active. Initially, the temperature of the hydrogenation reaction was varied in 20 degree increments from 0 to 80 °C, and the results are shown in Figure 3a. The observed rate of the reaction increased somewhat linearly with respect to temperature, with the maximum rate occurring at 60 °C. At the highest temperature studied (80 °C), there was a substantial decrease in activity, suggesting that deactivation of the catalyst was occurring. To allow for comparison among other known arene hydrogenation catalysts, the hydrogenation of toluene was examined, in triplicate, between 0 and 40 °C to calculate the activation energy. The initial rates were measured during the first 30 min of the toluene hydrogenation reaction. The results were plotted in an Arrhenius plot (Figure 3b), and the activation energy was calculated to be 30.4 kJ/mol. This activation energy is moderate when compared to those previously reported for arene hydrogenation. Dupont et al., for instance, reported an activation energy of 42.0 kJ/mol for the hydrogenation of toluene with Ru NPs<sup>1</sup> and Somorjai et al. reported activation energies of 34.7 and 45.6 kJ/mol for benzene hydrogenation with cuboctahedral and cubic Pt NPs, respectively.<sup>2</sup>

The molar ratio of toluene to metal in the catalyst was varied at ratios of 50, 200, 500, and 1000, with the results shown in Figure 3c. The highest observed rates were obtained for the ratios of 200 and 500. When the ratio was further increased to 1000, there was a substantial decrease in activity, suggestive of substrate inhibition. Preliminary pressure studies were also done, and showed a relatively linear increase in reaction rate versus hydrogen pressure. (Supporting Information, Figure S5).

**Figure 4.** TEM images and particle size histograms of NP catalysts: (a) Rh<sub>0.5</sub>Pt<sub>0.5</sub>/Al<sub>2</sub>O<sub>3</sub>, (b) Ir<sub>0.5</sub>Pt<sub>0.5</sub>/Al<sub>2</sub>O<sub>3</sub>, (c) Ir<sub>0.5</sub>Rh<sub>0.5</sub>/Al<sub>2</sub>O<sub>3</sub>, (d) Ru<sub>0.5</sub>Pt<sub>0.5</sub>/Al<sub>2</sub>O<sub>3</sub>, (e) 0.5% Rh/Al<sub>2</sub>O<sub>3</sub>.

To determine the number of catalytically active sites present, and to allow for more accurate comparison of the activities of different catalysts, a series of CS<sub>2</sub> poisoning experiments were performed on the Rh<sub>0.5</sub>Pt<sub>0.5</sub>/Al<sub>2</sub>O<sub>3</sub> and 0.5% Rh/Al<sub>2</sub>O<sub>3</sub> catalysts in triplicate.<sup>91</sup> Known amounts

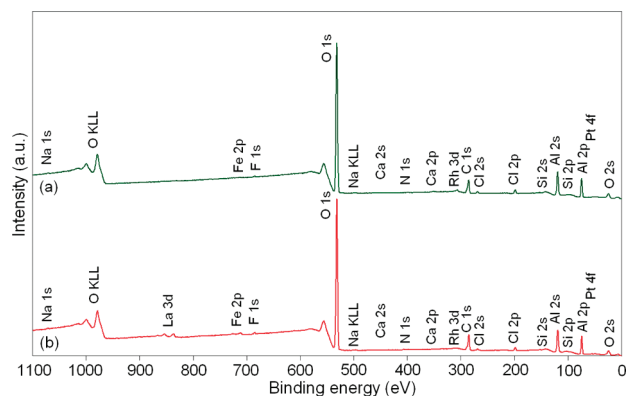


**Figure 5.** X-ray photoelectron spectra survey scans for  $\text{Rh}_{0.5}\text{Pt}_{0.5}/\text{Al}_2\text{O}_3$ . The spectra indicated in black (a) corresponds to the catalyst before the toluene hydrogenation reaction, and the spectra in red (b) corresponds to the catalyst after the toluene hydrogenation reaction.

of  $\text{CS}_2$  were added to the toluene hydrogenation reaction, and the activity of the catalysts was measured. The rates of the unpoisoned  $\text{Rh}_{0.5}\text{Pt}_{0.5}/\text{Al}_2\text{O}_3$  and 0.5%  $\text{Rh}/\text{Al}_2\text{O}_3$  catalysts were measured at 5 atm  $\text{H}_2$  and 295 K, and the results are shown in Table 2. Using these rates, the TOFs were calculated based on the molar amount of metal used, which was the same for the two different catalysts. As already shown in Table 2, the  $\text{Rh}_{0.5}\text{Pt}_{0.5}/\text{Al}_2\text{O}_3$  catalyst is more active, with a TOF of  $43.8 \text{ h}^{-1}$ , than the 0.5%  $\text{Rh}/\text{Al}_2\text{O}_3$  catalyst which has a TOF of  $27.2 \text{ h}^{-1}$ . Upon performing the poisoning studies, the amount of  $\text{CS}_2$  required to completely deactivate each catalyst was calculated to be  $0.081 \text{ mol CS}_2/\text{mol total metal}$  for the  $\text{Rh}_{0.5}\text{Pt}_{0.5}/\text{Al}_2\text{O}_3$  catalyst and  $0.046 \text{ mol CS}_2/\text{mol total metal}$  for the 0.5%  $\text{Rh}/\text{Al}_2\text{O}_3$  catalyst (Supporting Information, Figure S6). The higher value for the  $\text{Rh}_{0.5}\text{Pt}_{0.5}/\text{Al}_2\text{O}_3$  catalyst suggests that there are more catalytically active sites present in this bimetallic catalyst than in the commercial catalyst. Hornstein et al. assumed a 1/5 poison to metal-atom stoichiometry ratio to calculate corrected TOF values for each catalyst.<sup>91</sup> On the basis of this assumption, the corrected TOFs for the  $\text{Rh}_{0.5}\text{Pt}_{0.5}/\text{Al}_2\text{O}_3$  and the 0.5%  $\text{Rh}/\text{Al}_2\text{O}_3$  catalysts are  $108 \text{ h}^{-1}$  and  $118 \text{ h}^{-1}$ , respectively. Although these values for the corrected TOFs are similar, the need for a higher quantity of catalyst poison ( $\text{CS}_2$ ) for the bimetallic catalysts suggests that there are more active (but less reactive) sites than in the commercial 0.5%  $\text{Rh}/\text{Al}_2\text{O}_3$  catalyst.

**Characterization.** Since the synthesis is based upon a one pot in situ production of both the support and the NPs simultaneously, little is known about the morphology or structure of the resulting catalyst. From the TEM image of  $\text{Rh}_{0.5}\text{Pt}_{0.5}/\text{Al}_2\text{O}_3$  catalyst (Figure 4a) the size of the NPs was measured to be  $3.1 \pm 1.0 \text{ nm}$ . When TEM images were obtained upon the completion of the hydrogenation reaction using the  $\text{Rh}_{0.5}\text{Pt}_{0.5}/\text{Al}_2\text{O}_3$  catalyst, the size of the NPs was measured to be  $3.3 \pm 1.1 \text{ nm}$ , indicating no significant change in size or morphology of the NPs during the course of the reaction (Supporting Information, Figure S7). The size of the NPs in the  $\text{Ir}_{0.5}\text{Pt}_{0.5}/\text{Al}_2\text{O}_3$  catalyst was measured to be  $2.9 \pm 0.9 \text{ nm}$  (Figure 4b),  $3.8 \pm 1.2 \text{ nm}$  for the  $\text{Ir}_{0.5}\text{Rh}_{0.5}/\text{Al}_2\text{O}_3$  catalyst (Figure 4c),  $4.2 \pm 1.5 \text{ nm}$  for the  $\text{Ru}_{0.5}\text{Pt}_{0.5}/\text{Al}_2\text{O}_3$

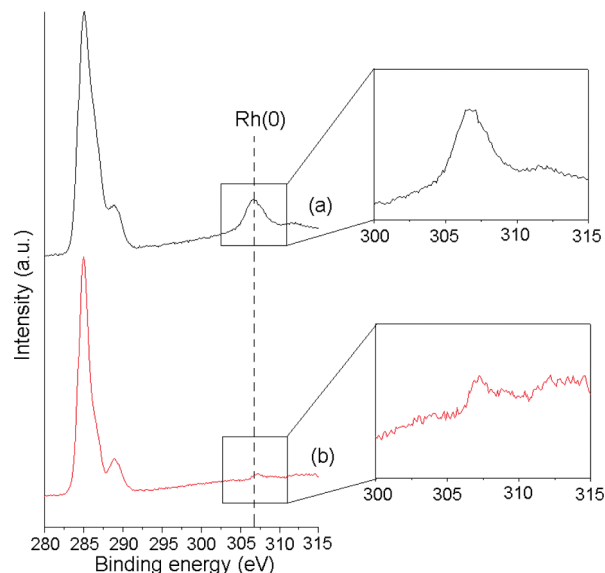


**Figure 6.** High-resolution XPS of the Rh 3d peak in  $\text{Rh}_{0.5}\text{Pt}_{0.5}/\text{Al}_2\text{O}_3$ . The spectra indicated in black (a) is before the toluene hydrogenation reaction and the spectra indicated in red (b) is after the toluene hydrogenation reaction. The binding energy for Rh 3d before and after reaction are 306.7 and 307.1 eV, respectively.

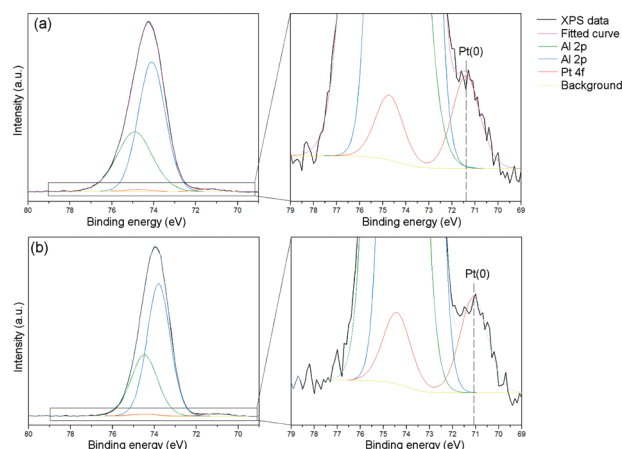


**Figure 7.** High-resolution XPS of Pt in  $\text{Rh}_{0.5}\text{Pt}_{0.5}/\text{Al}_2\text{O}_3$ . The spectra indicated in (a) are before the toluene hydrogenation reaction, and the spectra indicated in (b) are after the toluene hydrogenation reaction. The BE for Pt before and after reaction are 71.4 and 71.2 eV, respectively.

catalyst (Figure 4d), and  $5.2 \pm 1.6 \text{ nm}$  for the commercial 0.5%  $\text{Rh}/\text{Al}_2\text{O}_3$  catalyst (Figure 4e).

XPS analysis of the  $\text{Rh}_{0.5}\text{Pt}_{0.5}/\text{Al}_2\text{O}_3$  catalyst was performed to determine the oxidation states of the two metals present in the catalyst. The survey scan shown in Figure 5 shows the XPS spectra before (spectra shown in black) and after (spectra shown in red) the toluene hydrogenation reaction. The two spectra are very similar, and the Rh 3d, Al 2s, Al 2p, and Pt 4f peaks can be clearly identified in both, though the Al 2p and Pt 4f peaks overlap.

From the high-resolution spectra of Rh in  $\text{Rh}_{0.5}\text{Pt}_{0.5}/\text{Al}_2\text{O}_3$  (Figure 6) the binding energy (BE) of Rh was measured to be 306.7 eV before the reaction and 307.1 eV after the reaction. From the high-resolution spectra of Pt in  $\text{Rh}_{0.5}\text{Pt}_{0.5}/\text{Al}_2\text{O}_3$  (Figure 7), a curve-fitting program was used to obtain information about the Pt 4f peak since it overlaps with the Al 2p peak. The BE of Pt was



determined to be 71.4 eV before the hydrogenation and 71.2 eV after the hydrogenation. By considering the BE of the Rh and Pt peaks before and after the hydrogenation reactions, it can be seen that there was no substantial deviation in the BE before and after the hydrogenation, suggesting that the oxidation state of the metal does not change substantially.

XPS spectra were also obtained for the 0.5% Rh/ $\text{Al}_2\text{O}_3$ ,  $\text{Ru}_{0.5}\text{Pt}_{0.5}/\text{Al}_2\text{O}_3$ ,  $\text{Ir}_{0.5}\text{Pt}_{0.5}/\text{Al}_2\text{O}_3$ , and  $\text{Ir}_{0.5}\text{Rh}_{0.5}/\text{Al}_2\text{O}_3$  catalysts. For the commercial catalyst, 0.5% Rh/ $\text{Al}_2\text{O}_3$ , the high resolution XPS spectra showed a BE of 308.8 eV for Rh (Supporting Information, Figure S9), suggesting that the Rh was oxidized to Rh(III). For  $\text{Ru}_{0.5}\text{Pt}_{0.5}/\text{Al}_2\text{O}_3$  (Supporting Information, Figures S10 and S11), the BE for Ru was 280.1 and 71.2 eV for Pt, indicating that both metals are in the zero oxidation state. From the high-resolution spectra for  $\text{Ir}_{0.5}\text{Pt}_{0.5}/\text{Al}_2\text{O}_3$  (Supporting Information, Figures S12 and S13) the BE for Ir was 60.7 and 71.4 eV for Pt, indicating that both metals were in the zero oxidation states. For  $\text{Ir}_{0.5}\text{Rh}_{0.5}/\text{Al}_2\text{O}_3$  (Supporting Information, Figures S14 and S15), the BE for Ir and Rh were 60.4 and 306.7 eV, respectively, corresponding to the zero oxidation states for both metals.

Since acid-catalyzed sol–gel syntheses are known to give high-surface area metal oxides,<sup>99</sup> BET measurements were performed to measure the surface area of the blank support and the catalyst. The surface area of the blank support was measured to be 434  $\text{m}^2/\text{g}$ , which is in the range of surface areas reported in the literature for alumina.<sup>100,101</sup> The surface area of the  $\text{Rh}_{0.5}\text{Pt}_{0.5}/\text{Al}_2\text{O}_3$  catalyst was measured to be 557  $\text{m}^2/\text{g}$  (Supporting Information, Figure S16).

(99) Fahlman, B. D. *Materials Chemistry*; Springer: New York, 2007.

(100) Ennas, G.; Falqui, A.; Paschina, G.; Marongiu, G. *Chem. Mater.* **2005**, *17*, 6486–6491.

(101) Corrias, A.; Casula, M. F.; Falqui, A.; Paschina, G. *Chem. Mater.* **2004**, *16*, 3130–3138.

## Conclusions

Through a simple screening approach, four active bimetallic catalysts (RhPt, RuPt, IrPt, and IrRh) were identified. Through confirmation of the results in bulk,  $\text{Rh}_{0.5}\text{Pt}_{0.5}/\text{Al}_2\text{O}_3$  was found to be the most active catalyst, which was then tested under a variety of parameters, and the activation energy was measured to be 30.4 kJ/mol. Through the use of standard materials characterization techniques, all of the bimetallic catalysts were determined to consist of small, zero oxidation state NPs that were well dispersed throughout the alumina supports. Future work on this project will involve screening trimetallic combinations for catalytic activity, and screening for activity on mixed metal oxide supports and in the presence of sulfur and nitrogen containing compounds.

**Acknowledgment.** The Alberta Ingenuity–Imperial Oil Centre for Oil Sands Innovation (COSI), NINT-NRC, the University of Alberta and CRC programs are thanked for their generous financial support. Dr. Mike Xia of the NINT Chemical Analysis Lab is thanked for performing the GC-MS analysis and obtaining the BET measurements. The staff of the Department of Chemistry Glass Shop are thanked for making the sample holders. Jian Chan and Peng Li from the NINT Electron Microscopy Lab are thanked for obtaining the TEM images. Shihong Xu from the Alberta Centre for Surface Engineering and Science (ACES) is thanked for obtaining the XPS data.

**Supporting Information Available:** Images of sample holders and set up; plot of comparison of trends observed through screening with those observed in batch; plot of observed rate versus moles of  $\text{CS}_2$ /moles of total metal for the hydrogenation of toluene by  $\text{Rh}_{0.5}\text{Pt}_{0.5}/\text{Al}_2\text{O}_3$  and 0.5% Rh/ $\text{Al}_2\text{O}_3$ ; TEM image and histogram of  $\text{Rh}_{0.5}\text{Pt}_{0.5}/\text{Al}_2\text{O}_3$  NPs after the hydrogenation of toluene; XPS spectra of  $\text{Ir}_{0.5}\text{Pt}_{0.5}/\text{Al}_2\text{O}_3$ ,  $\text{Ru}_{0.5}\text{Pt}_{0.5}/\text{Al}_2\text{O}_3$ ,  $\text{Ir}_{0.5}\text{Rh}_{0.5}/\text{Al}_2\text{O}_3$ , and 0.5% Rh/ $\text{Al}_2\text{O}_3$  catalysts; the 5-point BET surface area plot. This material is available free of charge via the Internet at <http://pubs.acs.org>.